Circuit and Numerical Modeling of Electrostatic Discharge Generators

Spartaco Caniggia, *Member, IEEE*, and Francescaromana Maradei, *Senior Member, IEEE*

***Abstract*—This paper provides two accurate and efficient models of electrostatic discharge generators which permit to reproduce the discharge current in the contact mode, taking into account the load effect. The first model is based on a circuit approach and is suitable to be implemented in any commercial circuit simulator. The second model is based on the numerical solution of the field equations by using the commercial numerical-code microwave studio based on the finite-integration technique. The validation of the proposed circuit and numerical models is carried out by comparison with measurements.**

***Index Terms*—Electromagnetic compatibility (EMC), electromagnetic interference (EMI), electrostatic discharge (ESD), ESD generator, immunity, numerical modeling, numerical simulations.**

I. Introduction

ELECTROSTATIC discharge (ESD) is a severe source of interference which can produce damages, upset, or failures in electronic systems. This problem is receiving more and more concern especially in the light of increasing operating speed as well as decreasing operating voltage of electronic components [1], [2]. The effects produced by ESD are usually observed by separating conducted interference (i.e., direct effect) due to the direct injection of the discharge current in the victim device, and radiated interference (i.e., indirect effect) related to the coupling with the electromagnetic field radiated by the ESD event. ESD on electronic devices can occur when the device itself become charged by triboelectrification and approaches another conductor or while a human charged by triboelectrification handles the device. Charge accumulation by triboelectrification or induction process is at the origin of any ESD event. Several studies have been addressed to investigate the parameters that influence the charge accumulation and discharge process in some basic discharge geometries [3]–[8].

Over the years, a great effort has been addressed by the scientific community to establish ESD standard procedures suitable to test electrical and electronic systems immunity, assuring repeatable and reproducible results [9]. To this aim, an important role has been played by several studies on ESD current waveform, focusing the attention to the amplitude and rise-time variations due to different voltages, approach speeds, and electrode shapes [10]–[14]. The standard International Electrotechnical Commission (IEC) 61000-4-2 [9] defines the typical waveform of the discharge current, range of test levels, test equipment including specifications for test generator, test setup, and test procedures.

ESD generators are widely used for testing the immunity of electronic equipment and permit to reproduce typical human-metal ESD events. To ensure the reproducibility of test results, the majority of available ESD generators are built in compliance with the specifications of the IEC 61 000-4-2 standard [9] and its second edition, which is still under discussion. A crucial point still under discussion is with regard to the characteristics and performance of the ESD generators in order to avoid the great differences in the current waveforms caused by ringing after the first peak [15], [16]. The standard [9] defines two methods of ESD testing: contact and air discharge methods. In the contact discharge method, the electrode of the test generator is held in contact with the equipment under test (EUT) and the discharge actuated by the discharge switch within the generator. In the air discharge method, the charged electrode of the test generator is brought close to the EUT and the discharge actuated by a spark to the ground plane. This second method is characterized by a low reproducibility [12], [13].

The immunity prediction of electric and electronic equipment against ESD events by experimental activity is not considered to be very practical in particular when the evaluations is required for different design choices. For this reason, in the last few years, a great concern has been addressed by many researches to the numerical simulation of ESD events [17]–[20]. A numerical model based on the finite-difference time-domain (FDTD) method adopting impedance network boundary conditions was proposed in [17] to predict the ESD effects inside penetrable conductive enclosures. Recently, numerical models based on the FDTD method of typical ESD generators have been presented in order to simulate current discharge and radiated fields [18], [19]. In the past, an analytic approach based on transmission line formulation was proposed to predict voltage induced into a coaxial cable by an ESD discharge [20]. In [20], the ESD was simulated by a current source without taking into account the load effect of the ESD generator. As the same authors recognize, this procedure brings to an overestimation of the subsequent peaks of the induced disturb. The effects of the variation in the impedance elements of the discharge path on the peak value and rise time of the discharge are also highlighted in [3], [21], and [22].

Paper MSDAD-06-13, presented at the 2005 Industry Applications Society Annual Meeting, Hong Kong, October 2–6, and approved for publication in the IEEE TRANSACTIONS ON INDUSTRY APPLICATIONS by the Electrostatic Processes Committee of the IEEE Industry Applications Society. Manuscript submitted for review October 15, 2005 and released for publication July 24, 2006. This work was supported by Italtel S.p.A.

S. Caniggia is at Viale Morandi 7, 20010 Bareggio, Italy (e-mail: spartaco.caniggia@ieee.org).

F. Maradei is with the Department of Electrical Engineering, University of Rome "La Sapienza," 00184 Rome, Italy (e-mail: fr.maradei@ieee.org).

Color versions of all figures are available online at http://ieeexplore.ieee.org.

Digital Object Identifier 10.1109/TIA.2006.882686

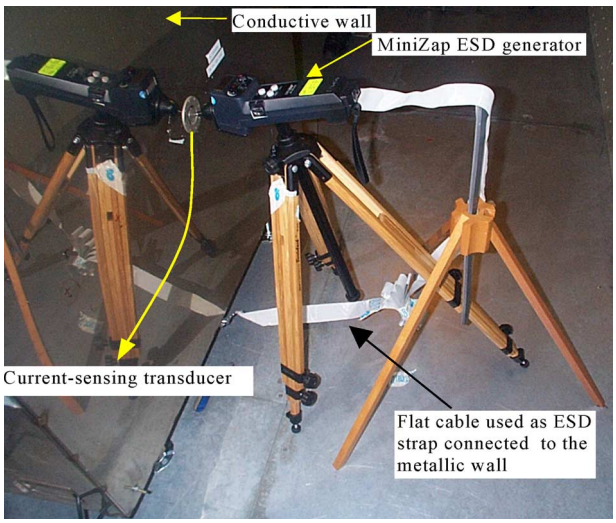

Fig. 1. Test setup used for ESD current calibration.

The great concern on numerical simulation of ESD testing is even testified by the working group involved in drawing up the new version of the IEC standard since the possibility to allow ESD immunity certifications by suitable and reliable numerical tools is very appealing. In this framework, a topical point is to get ready accurate models for the ESD generator suitable to account for the load effect of the generator. This paper provides two accurate models of the ESD generator that allow modeling the discharge current in the contact mode, taking into account the load effect. In the first model, the ESD generator is modeled by an electric circuit suitable to be implemented in any commercial circuit simulator. The second model is based on the three-dimensional (3-D) numerical simulation of the ESD generator by the commercial tool microwave studio (MWS), based on the finite-integration technique [23], [24]. The validation of both models is made by comparison with the measurements, by using the test setup for current calibration reported in [9]. Both the proposed ESD generators are then used to predict immunity in a coaxial cable connecting two devices inside enclosures.

II. Description of Experimental Setup for ESD Current Calibration

The test setup for current calibration arranged in the shielded room of Italtel S.p.A, in accordance with IEC 61 000-4-2 standard [9], is shown in Fig. 1. This test setup models the ESD event on a conductive wall. The measurement of the ESD current is performed by using the current-sensing transducer, which is shown in Fig. 1. The constructional details of the resistive load behaving as current transducer are described in detail in the standard [9].

The wall is a side of a shielded enclosure in which the target is mounted to measure currents using a digital oscilloscope within the enclosure. This configuration permits to avoid the coupling between the ESD event and the instrumentation. All the measurements were carried out at a charging voltage of the ESD generator of 5 kV and with an oscilloscope characterized by a 2-GHz bandwidth. The flat cable used as the ESD strap is connected to the metallic wall where the discharge occurs.

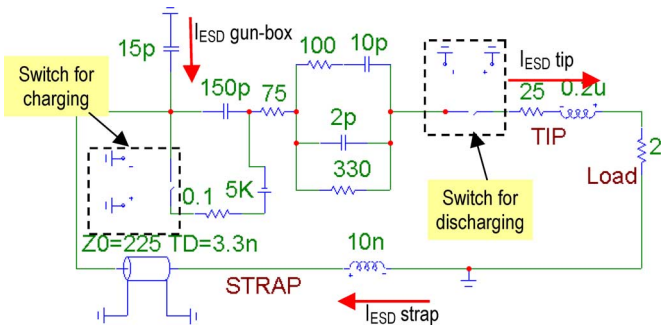

Fig. 2. SPICE equivalent circuit of a typical ESD generator.

The strap current has been measured using a setup similar to the one shown in Fig. 1, where the positions of the discharge point and of the ground strap connection have been swapped.

III. Model of ESD Generator

A. Equivalent Circuit Model

The purpose of an ESD generator is to reproduce typical human-metal ESD. Considering this, a suitable circuital equivalent model could be the one shown in Fig. 2. This circuit model can be easily implemented in any SPICE-based circuit simulator [25]. The lumped circuital elements are chosen as typical values that simulate the body and the arm effects of the person that causes ESD. Concerning the values of circuit elements in Fig. 2, the 150-pF capacitance and the 330-Ω resistance are defined in the IEC 61000-4-2 standard, while the other parameters were chosen in order to reproduce the reference waveform of the discharge current according to the analytical expression defined in [16].

In the circuit model of Fig. 2, there are two switches: The first one (on the left side) is used to charge the 150-pF capacitor at the typical voltage of 5 kV; the second switch (on the right side) provides the discharge. The flat cable used as the ESD strap connected to the ground is modeled by the series connection of the lossless transmission line characterized by a characteristic impedance of 225 Ω, a propagation time of 3.3 ns, and a 10-nH inductance which models the wire used to connect the flat cable with the metallic wall. The characteristic impedance and delay of the strap were analytically calculated [28] by considering the horizontal and vertical path of the strap as a conductor above a ground plane, where the reference plane was the metallic floor of the chamber and the metallic wall of the point of discharge, respectively. The 10-nH inductance was estimated applying the partial-inductance concept for a segment of a loop [28], where the loop is formed by the ESD gun and flat cable. The 15-pF capacitance models the capacitive coupling between the ESD gun and the metallic wall (see the experimental setup shown in Fig. 1). The ESD tip is modeled by the series of a 25-Ω resistance with the 0.2-μH inductance. It should be noted that the load represents the impedance of the target [9] and, in the considered simulation, is given by a 2-Ω resistance.

B. Full-Wave Model

The ESD generator is modeled by using the commercial numerical code MWS based on the finite-integration technique

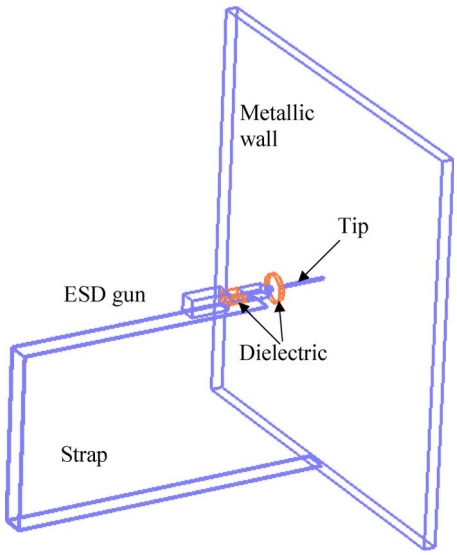

Fig. 3. ESD simulator modeled in MWS.

[23], [24]. The model, shown in Fig. 3, contains dielectric parts, metallic parts, and lumped circuit elements which permit to reproduce the physical form of a typical ESD generator and the reference discharge current [16].

The geometrical configuration of the ESD generator adopted for the numerical simulation is similar to that of the DITO gun by Amplifier Research [19], [26]. Details on the material properties used to model the different part of the ESD gun are shown in Fig. 4. The lumped circuit elements adopted in the MWS model are shown in Fig. 5. The model is excited at port 2 (see Fig. 5) by an ideal current source with 25 Ω, assuming a step rise time of 1 ns to reproduce the actual slow charging, switching, and rapid discharge process of an ESD generator in contact mode.

IV. Validation of ESD Generator Models

To verify whether the proposed models are suitable to simulate a typical commercial ESD generator, the current on the tip and on the strap were measured by using the setup for current calibration described in Section II.

The tip and strap currents obtained by the two proposed models are shown in Figs. 6 and 7. The comparison between the simulation results and the measurements reveals a very good accuracy. Moreover, the following considerations can be done.

1) The first fast rise time (less than 1 ns) is reproduced and matched well with the reference IEC current.
2) The measured and simulated waveforms after the first peak follow quite well with slight oscillations of the reference IEC current. This is mainly due to the length and orientation of the strap.
3) The current on the strap has a slower rise time than the current on the tip. This is due to the capacitance between the ESD generator and the environment (the metallic wall in this case, see the 15 pF of Fig. 2) that permits an alternative path for the first peak of the ESD current.

In order to verify the generality of the developed models in terms of reproducibility of test results even using different

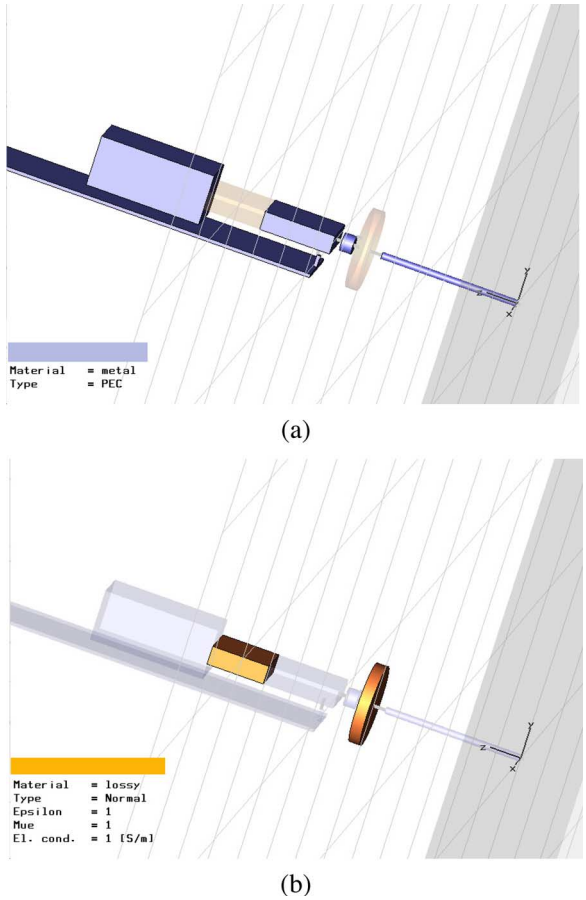

Fig. 4. Material details of the ESD simulator model in MWS. (a) Perfect electric conductive and (b) lossy dielectric regions.

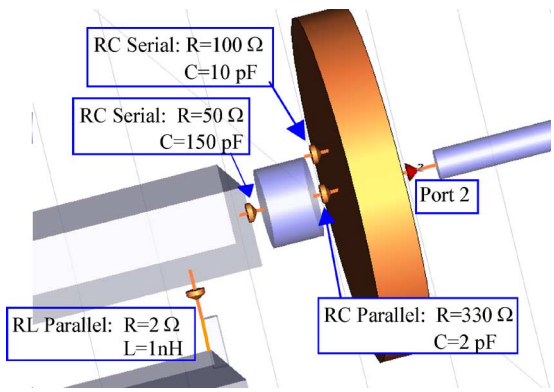

Fig. 5. Lumped-element network and port excitation used to reproduce the physical form of a typical ESD generator and the reference discharge current proposed.

ESD gun, the tip current has been measured several time by using the MiniZap gun by Thermo Electron Corporation Fig. 8(a) [27] and by using the DITO gun [26] Fig. 8(b). The measured tip currents shown in Fig. 9 show that there is a very little difference between the two measurements obtained using MiniZap gun and with that obtained using DITO gun. In particular, it should be noted that the rise times to get the first peak of the waveform are very close, and this is a fundamental requirement for calibration since the first peak is the most critical under the electromagnetic interference (EMI point of

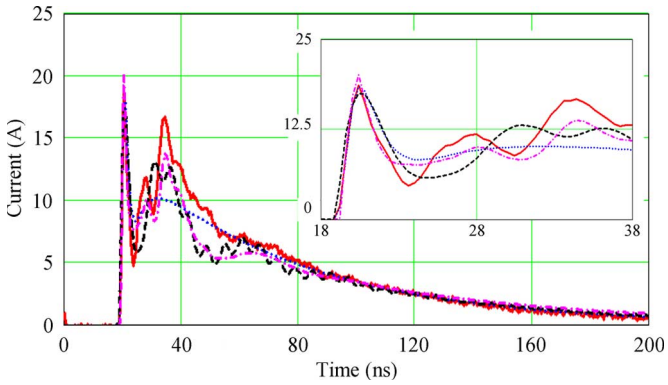

Fig. 6. Tip current: measured (solid line); standard IEC (dot line); SPICE-like equivalent circuit (dashed line); and MWS model (dashed-dot line).

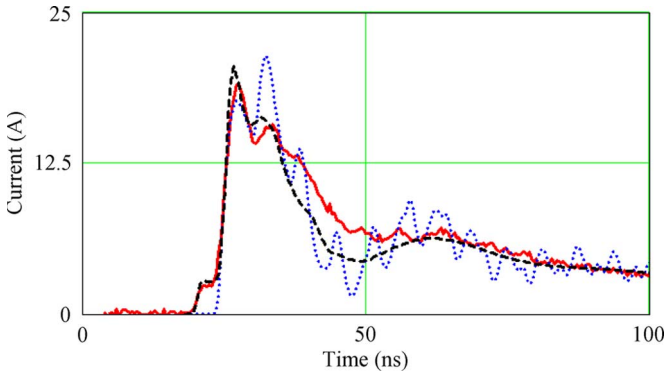

Fig. 7. Strap current: measured (solid line); SPICE-like equivalent circuit (dashed line); and MWS model (dashed-dotted line).

(a)

(b)

Fig. 8. ESD generators. (a) MiniZap and (b) DITO guns.

view. Differences can be noted on the subsequent ringing due to the construction of the gun and the position of the strap. This is a typical characteristic of many commercial ESD generators. To limit these differences, new specifications are under study inside the working group in charge to prepare the new IEC standard for ESD [15], [16].

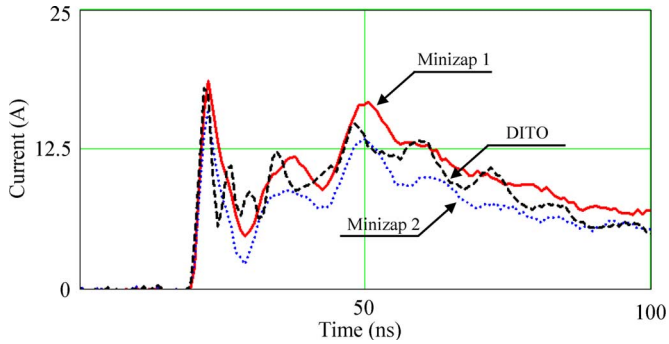

Fig. 9. Measured tip current: MiniZap 1 (solid line); MiniZap 2 (dot line); and DITO (dashed line).

V. ESD on a Test Cable

To test the generality of the developed models, they are used to predict the induced ESD effects in a coaxial cable installed in typical configuration. The test setup used for measurements is shown in Fig. 10. An RG58 coaxial cable was used as test cable, with the shield connected using a BNC connector at one end of a metal box with a Tektronix TDS 684B oscilloscope inside (on the left). The left-hand enclosure of size $1 \times 1.2 \times 1.5$ m is placed at 15 cm above the metallic floor of the shielded room for EMC tests and grounded by four metallic straps positioned at the four angles of the box. At the other end (on the right), the shield of the cable was clamped to a small shielded box in direct contact with the metallic floor.

The RG-58 coaxial cable has the following parameters: characteristic impedance Zo $= 50\ \Omega$, internal dielectric permittivity $\varepsilon_{\rm r} = 2.3$, internal wire radius $r_{\rm w} = 0.394$ mm, internal shield radius $r_{\rm s} = 1.397$ mm, and shield thickness $t = 0.127$ mm. The RG-58 cable of length $L = 3$ m (total length connector-to-connector $= 3.4$ m) is placed at $h = 6$ cm above the ground plane. The inner wire of the coaxial cable was terminated at the left side by the input impedance of the oscilloscope (50 Ω) and at the right side by a resistance of the same value.

Several discharges at 5 kV in contact mode were performed in different points of the enclosure containing the oscilloscope. The most sever ESD event is the one that occurred on the connector of the coaxial cable, as shown in Fig. 11.

A. Prediction of Induced Effects Using the ESD Generator Circuit Model

The compact equivalent circuit of the box–cable–box structure used to predict the measured waveforms with a full circuit approach is illustrated in Fig. 12, where the 50-Ω terminations of the cable inner wire and those used to model the cable shield connections to the ground are clearly highlighted. In particular, on the right-end side, the cable shield connection to the box in direct contact with the ground is modeled by a 1-Ω resistance. The shield cable connection to the enclosure grounded by four metallic straps occurring on the left-end side is modeled by the RLC network shown in Fig. 12, where the capacitance $C_{\rm bg} = 34.2$ pF was estimated by a static finite-element numerical code for 3-D structure and the inductance $L_{\rm bgc} = 11.2$ nH was analytically estimated, considering the shape of the four straps used to connect the box to the ground and applying

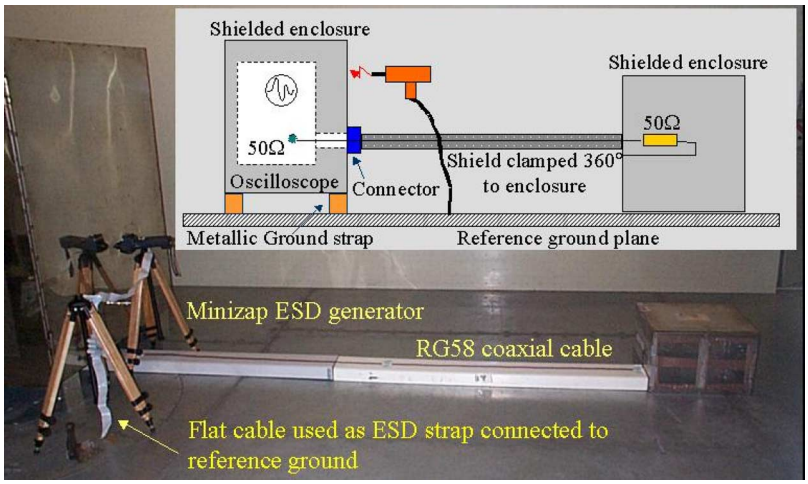

Fig. 10. Test setup used for measuring ESD disturbance in a coaxial cable.

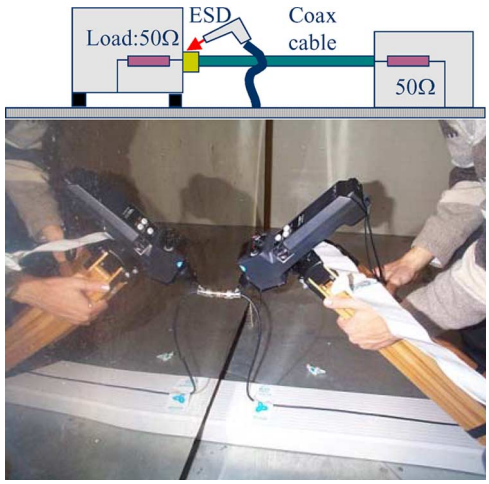

Fig. 11. ESD current injected on the cable connector.

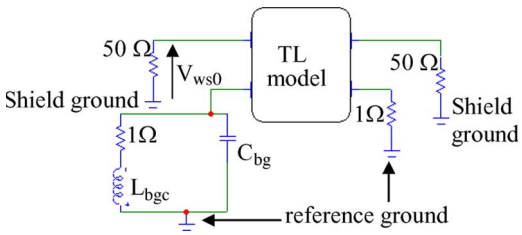

Fig. 12. Equivalent circuit of the box-to-box structure under test.

the partial-inductance concept [28]. It should be noted that the correct modeling of the left-enclosure ground connection is of the utmost importance to achieve accurate results.

The coaxial-cable transmission line of Fig. 12 has been modeled by the SPICE-like circuit model proposed in [29]. This model is based on the discretization of the cable line in a series cascade of line sections with time-constant lumped parameters, derived by the vector fitting technique for the time-domain modeling of the frequency dependent losses. Details on the cable circuit model and its derivation can be found in [29].

The wire-to-shield induced voltage at $x = 0$ (i.e., V_{ws0} in Fig. 12) is calculated by adopting 68 cells of 5 cm to discretize a 3-m long coaxial cable and by assuming that the point of

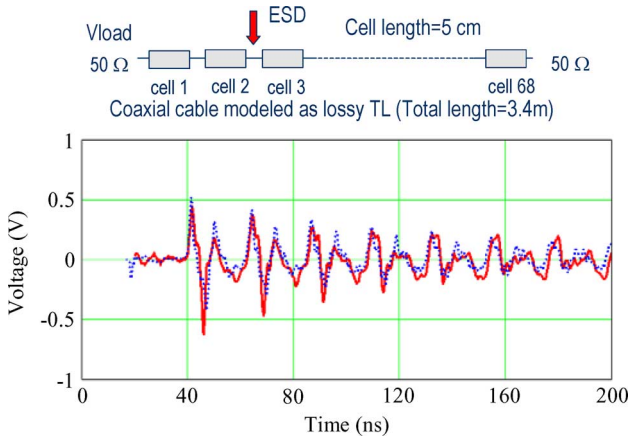

Fig. 13. Voltage V_{ws0} on the 50-Ω left-end load for a coaxial cable of length 3 m when the ESD event occurs on the cable connector: measured (solid line) and SPICE-like equivalent circuit (dotted line).

discharge was after two cells. The comparison between the calculated induced voltage V_{ws0} and the measurements is shown in Fig. 13, and a satisfactory agreement can be observed. It should be noted that the circuit simulation runs in few seconds in a computer with frequency clock of 800 MHz. Concerning the results, the following can be observed.

1) The rise times, the values, and the duration of the main peaks are reproduced quite well.
2) Some slight differences on the waveforms between the peaks are due to length and position of the strap.

The ESD-induced effects that occurred when the discharge point is on the box at the opposite side of the cable connector (no radiation effects) are shown in Fig. 14. Also in this case, the results obtained by the circuit simulator are in good agreement with the measurements. It should be noted that the worst case disturbance takes place when the discharge is on the connector and the enclosure on the left side is floating, as shown in Fig. 15. In this case, the box-to-ground connection has been modeled for simplicity by a lumped capacitance only. This could explain the discrepancies occurring after the first 50 ns, mainly due to the structure of the box-cable resonance and possible unmodeled further stray capacitance. By the way, the first peak, which is

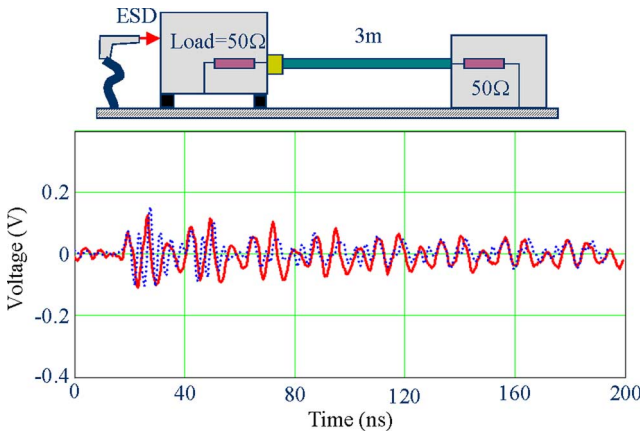

Fig. 14. Voltage V_{ws0} on the 50-Ω left-end load for a coaxial cable of length 3 m when the ESD event occurs on the box: measured (solid line) and SPICE-like equivalent circuit (dotted line).

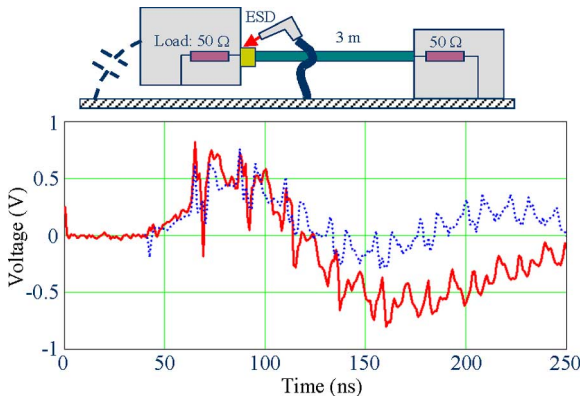

Fig. 15. Voltage V_{ws0} on the 50-Ω left-end load for a coaxial cable of length 3 m when the ESD event occurs on the connector and the box is floating: measured (solid line) and SPICE-like equivalent circuit (dotted line).

the most critical for the immunity, is predicted with a very good agreement.

B. Prediction of Induced Effects Using the ESD Generator Full-Wave Model

The prediction of the ESD-induced effects in the considered shielded-cable configuration, shown in Fig. 10, cannot be performed by any 3-D commercial numerical codes since none of them allow the simulation of the shielded-cable transfer impedance. Therefore, to calculate the wire-to-shield disturbance, a two-step procedure is proposed here.

Step 1) The current distribution on the shield of the cable due to the ESD discharge occurring at any point of the box where the cable is attached is calculated by a 3-D full-wave EM modeling technique. The ESD event on the coaxial-cable connector is modeled by MWS, and the tangential magnetic-field distribution on the cable shield is obtained through the definition of several magnetic-field probes, as illustrated in Fig. 16. The current distribution along the shield is then derived by Amper's law $I_{\mathrm{sh}} = 2\pi r_{\mathrm{se}}$ H, where r_{se} is the shield external radius. The calculated currents at regular steps are stored in files.

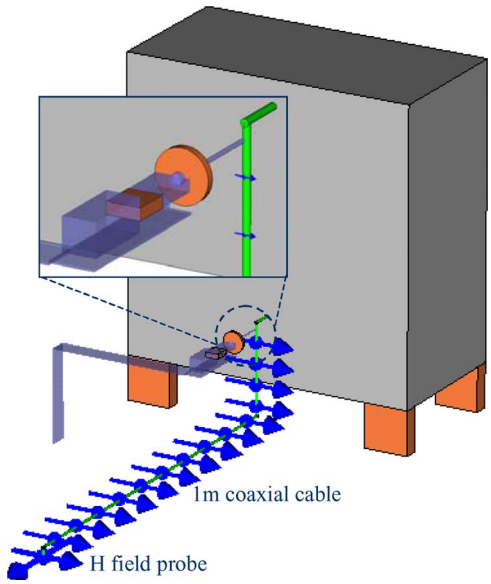

Fig. 16. Structure under test simulated with MWS.

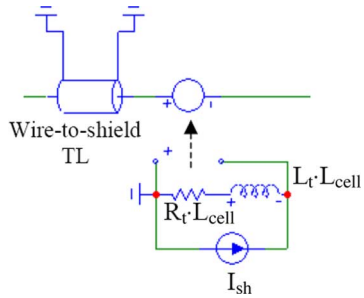

Fig. 17. Lossless line equivalent circuit of one cell of the coaxial-cable wire-to-shield mesh.

Step 2) The induced wire-to-shield voltage is obtained by a circuit approach using the calculated current distribution on the cable shield and the transfer impedance concept [30]. Adopting the simplified expression $Z_{\mathrm{t}} = R_{\mathrm{t}} + j\omega L_{\mathrm{t}}$ for the transfer impedance, the wire-to-shield equivalent circuit of a lossless cable section of length L_{cell} can be represented, as shown in Fig. 17.

The comparison among measurements, the numerical-circuital MWS-SPICE procedure described in this section, and the SPICE-like model described in the previous section are shown in Fig. 18. It is interesting to note that the first peak of MWS-SPICE simulation is higher than the other two results because only 14 cells where used instead of 30 cells for the full circuit model to allow fast prediction.

VI. Conclusion and Discussion

Circuit and numerical models of an ESD generator have been proposed. The circuit model is suitable for implementation in any commercial circuit simulator such as SPICE. The numerical model is based on the 3-D simulation by the commercial tool MWS using the finite-integration technique. Both models allow the accurate simulation of the discharge current in the contact mode, taking into account the load effect of the ESD generator.

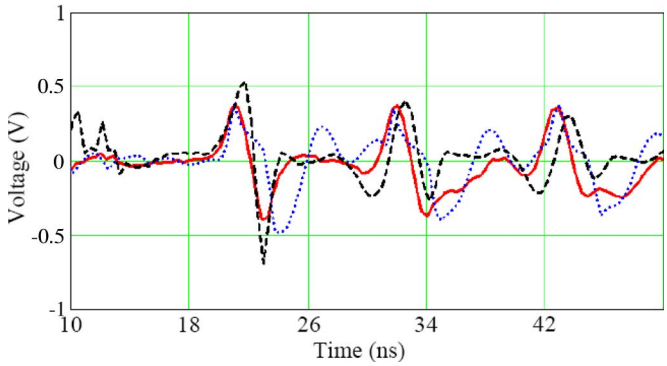

Fig. 18. Wire-to-shield voltage V_{ws0} on the 50-Ω left-end load for a coaxial cable of length 1 m when the ESD event occurs on the cable connector: measured (solid line); SPICE (dotted line); and MWS-SPICE (dashed line).

The efficiency of both models has been confirmed by the satisfactory agreement between simulation and measurements achieved in the setup configuration for the current calibration defined in the IEC 61 0000-4-2 [9].

The two models are complementary and can be employed to verify ESD reliability of electrical and electronic equipment, depending on the possibility to use or not a circuit approach to model the DUT. In case of ESD on a test cable connecting two devices as considered in Section V, the circuit approach can be applied if the cable has a well-defined distance from the reference plane and this distance is electrically short. In this case, the cable above a ground plane can be modeled by multiconductor transmission line model, and an efficient SPICE circuit can be drawn. The circuit approach fails when the cable has an electrically long distance from the reference plane (i.e., greater than 1/10 of the minimum wavelength of interest). In this case, the transmission line model is not valid anymore, and the combined numerical-circuit procedure presented in Section V-B should be used. In conclusion, the proposed MWS-SPICE procedure is appropriate when the cable has an irregular path and both the conducted and radiated interferences on the shield of the cable need to be considered. Applying this procedure, particular care should be addressed to assure line discretization into electrically short sections. It should be noted that the accuracy of the prediction model increases with the cell number as well as the time required for the simulation. Therefore, the right choice is a compromise between result accuracy and computational time.

The proposed models are of great interest since they represent an important item in the development of software tools suitable for the prediction of ESD immunity, especially during the design stage.

ACKNOWLEDGMENT

The authors would like to thank L. Vitucci for his significant support in the experimental measurements.

REFERENCES

[1] M.-D. Ker and K.-H. Lin, "The impact of low-holding-voltage issue in high-voltage CMOS technology and the design of latchup-free power-rail ESD clamp circuit for LCD driver ICs," *IEEE J. Solid-State Circuits*, vol. 40, no. 8, pp. 1751–1759, Aug. 2005.

[2] M.-D. Ker and W.-J. Chang, "ESD protection design of low-voltage-triggered p-n-p devices and their failure modes in mixed-voltage I/O interfaces with signal levels higher than VDD and lower than VSS," *IEEE Trans. Device Mater. Rel.*, vol. 5, no. 3, pp. 602–612, Sep. 2005.

[3] W. D. Greason, "Idealized model for charged device electrostatic discharge," *IEEE Trans. Ind. Appl.*, vol. 35, no. 1, pp. 240–258, Jan./Feb. 1999.

[4] ——, "Methodology for the characterization of the electrostatic discharge (ESD) event for bodies in approach," *IEEE Trans. Ind. Appl.*, vol. 37, no. 2, pp. 488–494, Mar./Apr. 2001.

[5] ——, "Analysis of electrostatic discharge for the human body and an automobile environment," *IEEE Trans. Ind. Appl.*, vol. 36, no. 2, pp. 517–525, Mar./Apr. 2000.

[6] W. D. Greason, I. M. Oltean, Z. Kucerowsky, and A. C. Nieta, "Triboelectric charging between polytetrafluoroethylene and metals," *IEEE Trans. Ind. Appl.*, vol. 40, no. 2, pp. 442–450, Mar./Apr. 2004.

[7] W. D. Greason, "Investigation of electrostatic discharge (ESD) for a three-body problem with small gaps," *IEEE Trans. Ind. Appl.*, vol. 42, no. 1, pp. 7–13, Jan./Feb. 2006.

[8] W. D. Greason and S. Bulach, "Constant energy device test for electrostatic discharge (ESD) of semiconductor devices," *IEEE Trans. Ind. Appl.*, vol. 33, no. 1, pp. 286–297, Jan./Feb. 1997.

[9] *Electromagnetic Compatibility (EMC) Part 4-2: Testing and Measurement Techniques—Section 2: Electrostactic Discharge (ESD) Immunity Test*, IEC-EN 61000-4-2, Sep. 1996.

[10] P. Richman, "Classification of ESD hand/metal current waves versus approach speed, voltage, electrode geometry and humidity," in *Proc. IEEE Symp. Electromagn. Compat.*, San Diego, CA, Sep. 1986, pp. 451–460.

[11] B. Daout, H. Ryser, A. Germond, and P. Zweiacker, "The correlation of rising slope and speed of approach in ESD tests," in *Proc. Int. Zurich Symp. Electromagn. Compat.*, Zurich, Switzerland, Mar. 1987, pp. 461–466.

[12] P. Richman, "Progress report on a different kind of ESD standard," in *Proc. Int. Zurich Symp. Electromagn. Compat.*, Zurich, Switzerland, Mar. 1989, pp. 349–354.

[13] D. Pommerenke, "ESD: Transient fields, arc simulation and rise time limit," *J. Electrostat.*, vol. 36, no. 1, pp. 31–54, Nov. 1995.

[14] ——, "ESD: Waveform calculation, field and current of human and simulator ESD," *J. Electrostat.*, vol. 38, no. 1, pp. 33–51, Oct. 1996.

[15] R. Chundru, D. Pommerenke, K. Wang, T. Van Doren, F. P. Centola, and J. S. Huang, "Characterization of human metal ESD reference discharge event and correlation of generator parameters to failure levels—Part I: Reference event," *IEEE Trans. Electromagn. Compat.*, vol. 46, no. 4, pp. 498–504, Nov. 2004.

[16] *Electromagnetic Compatibility (EMC) Part 4-2: Testing and Measurement Techniques—Section 2: Electrostactic Discharge (ESD) Immunity Test*, 77B/491/CD, IEC-EN 61000-4-2, Dec. 9, 2005.

[17] F. Maradei and M. Raugi, "Analysis of upset and failures due to ESD by the FDTD-INBCs method," *IEEE Trans. Ind. Appl.*, vol. 38, no. 4, pp. 1009–1017, Jul./Aug. 2002.

[18] K. Wang, D. Pommerenke, R. Chundru, T. Van Doren, J. Drewniak, and A. Shashindranath, "Numerical modeling of electrostatic discharge generators," *IEEE Trans. Electromagn. Compat.*, vol. 45, no. 2, pp. 258–271, May 2003.

[19] S. Caniggia, F. Centola, D. Pommerenke, K. Wang, and T. Van Doren, "ESD excitation model for susceptibility study," in *Proc. IEEE Symp. Electromagn. Compat.*, Boston, MA, Aug. 18–22, 2003, pp. 58–63.

[20] G. Cerri, R. De Leo, and V. M. Primiani, "ESD indirect coupling modeling," *IEEE Trans. Electromagn. Compat.*, vol. 38, no. 3, pp. 274–281, Aug. 1996.

[21] L. M. MacLeod and K. G. Balmain, "Compacted travelling wave physical simulator for human ESD," *IEEE Trans. Electromagn. Compat.*, vol. 39, no. 2, pp. 89–99, May 1997.

[22] D. Pommerenke and M. Aidam, "ESD: Waveform calculation, field and current of human and simulator ESD," *J. Electrostat.*, vol. 38, no. 1/2, pp. 33–51, Oct. 1996.

[23] T. Weiland, "A discretization method for the solution of Maxwell's equations for six-component fields," *Electron. Commun. AEU*, vol. 31, no. 3, pp. 116–120, 1977.

[24] Microwave Studio, Computer Simulation Technology (CST). [Online]. Available: www.cst.de

[25] Micrp-Cap 7, Spectrum Software. [Online]. Available: www.spectrum-soft.com

[26] DITO ESD Generator, Amplifier Research Worldwide. [Online]. Available: http://www.arww-rfmicro.com/html/18200.asp?id=258

[27] Key Tek MiniZap ESD Generator—Model MZ 15 EC, San Jose, CA: Termo Electron Corporation. [Online]. Available: http://www.thermo.com/com/cda/product/

[28] C. R. Paul, *Multiconductor Transmission Lines*. New York: Wiley, 1994.
[29] S. Caniggia, M. Feliziani, G. Manzi, and F. Maradei, "Time domain analysis of lossy shielded cables by CAD circuit simulators," in *Proc. IEEE Int. Symp. Electromagn. Compat.*, Santa Clara, CA, Aug. 9–13, 2004, pp. 952–957.
[30] M. Acquaroli, S. Caniggia, A. Giordano, and L. Vitucci, "Measurements and SPICE models for data lines under electrical fast-transient test," in *Proc. 4th Eur. Symp. EMC*, Brugge, Belgium, Sep. 11–15, 2000, pp. 357–362.

Spartaco Caniggia (M'98) was born in Venice, Italy, in 1948. He received the Laurea degree in electronic engineering from the University of Padua, Padua, Italy, in 1972.

After military service, he joined Italtel S.p.A. in 1975, where he has been involved in the various aspects of electrical phenomena in analog and digital devices, semiconductor development, and interconnection effects in high-speed ICs. He was the Chief of EMI/EMC and Physical Design in Business Unit-Products, Bareggio, Italy. He left Italtel at the end of 2004, and he currently is an EMC consultant. He has been a part-time Lecturer at the Universities of Rome "La Sapienza," L'Aquila, Milan, and Turin for signal integrity and EMC activities. He is also a member of the working group SC77B MT12 of the IEC regarding ESD. His areas of interest include the development of CAD tools and mathematical models for electrostatic discharge (ESD), shielding, grounding, and wiring, and methods for designing and testing telecommunication equipment to comply with EMC standards. He is the author or coauthor of more than 50 technical papers and reports on signal integrity, device and line modeling, and EMI problems in PCBs.

Dr. Caniggia received the 1996 Oral Presentation Second Best Paper Award at the IEEE International Symposium on Electromagnetic Compatibility, Santa Clara, CA.

Francescaromana Maradei (M'94–SM'06) was born in 1969. She received the Laurea degree in electrical engineering (*cum laude*) from University of Rome "La Sapienza," Rome, Italy, in 1992, the Diplome d'Etudes Approfondies (DEA) in electrical engineering from the Institut National Polytechnique de Grenoble, Laboratoire d'Electrotechnique de Grenoble, France, in 1993, and the Ph.D. degree in electrical engineering from the University of Rome "La Sapienza," in 1997.

She joined the Department of Electrical Engineering, University of Rome "La Sapienza," in 1996, where she is currently an Associate Professor. Her main interests are in numerical techniques and their application to EMC problems (shielding and transmission line analysis).

Dr. Maradei received the 2003 James Melcher Prize Paper Award from the IEEE TRANSACTIONS ON INDUSTRY APPLICATIONS, the Oral Presentation Best Paper Award at the International Symposium on Electromagnetic Compatibility—EMC ROMA 1994, Rome, Italy; and the Poster Presentation Best Paper Award at the International Symposium on Electromagnetic Compatibility—EMC EUROPE 2000, Brugge, Belgium. She is a member of the Board of Directors of the IEEE Electromagnetic Compatibility Society, where she is also serving as Chapter Coordinator. She served as an Associate Editor of the IEEE TRANSACTIONS ON ELECTROMAGNETIC COMPATIBILITY from 1999 to 2000. Since 1998, she has been a member of the Editorial Board of the IEEE Conference on Electromagnetic Field Computation (CEFC) and of the COMPUMAG Conference.